The Journal of Chemical Physics

Ionic mobility driven by correlated van der Waals and electrostatic forces

Cite as: J. Chem. Phys. **156**, 204501 (2022); https://doi.org/10.1063/5.0088835
Submitted: 20 February 2022 • Accepted: 05 May 2022 • Accepted Manuscript Online: 05 May 2022 • Published Online: 23 May 2022

Tuhin Samanta and Dmitry V. Matyushov

The Journal of Chemical Physics ARTICLE scitation.org/journal/jcp

Ionic mobility driven by correlated van der Waals and electrostatic forces

Cite as: J. Chem. Phys. 156, 204501 (2022); doi: 10.1063/5.0088835
Submitted: 20 February 2022 • Accepted: 5 May 2022 •
Published Online: 23 May 2022

Tuhin Samanta and Dmitry V. Matyushov[a)]

AFFILIATIONS

School of Molecular Sciences and Department of Physics, Arizona State University, P.O. Box 871604, Tempe, Arizona 85287-1604, USA

[a)]Author to whom correspondence should be addressed: dmitrym@asu.edu

ABSTRACT

Classical theories of dielectric friction make two critical assumptions: (i) friction due to van der Waals (vdW) forces is described by hydrodynamic drag and is independent of the ionic charge and (ii) vdW and electrostatic forces are statistically independent. Both assumptions turn out to be incorrect when tested against simulations of anions and cations with varying charge magnitude dissolved in water. Both the vdW and electrostatic components of the force variance scale linearly with the ionic charge squared. The two components are strongly anticorrelated producing simple relations for the total force variance in terms of self-variances. The inverse diffusion constant scales linearly with the charge squared. Solvation asymmetry between cations and anions extends to linear transport coefficients.

I. INTRODUCTION

The Kirkwood equation defines the diffusion constant for translational diffusion in terms of the variance of the stochastic force $\mathbf{F}$ acting on the particle and the relaxation time τ_F of the force–force autocorrelation function,[1]

$$D = (\beta\zeta)^{-1} = \left[(\beta^2/3)\langle(\delta\mathbf{F})^2\rangle\tau_F\right]^{-1}, \tag{1}$$

where $\delta\mathbf{F} = \mathbf{F} - \langle\mathbf{F}\rangle$ and $\beta = (k_BT)^{-1}$. The first equality is the Einstein equation connecting the diffusion constant to the friction coefficient ζ. The second equality (the Kirkwood equation) is an approximation since the memory time should replace τ_F in the exact result.[2] Deviations from the exact formula follow from a series expansion in the smallness parameter given by the square root of the ratio of the solvent and solute masses.[3] Recent molecular dynamics (MD) simulations have shown that the first nonvanishing correction is in fact quadratic in this smallness parameter and the first correction to the Kirkwood equation scales as the ratio of the solvent and solute masses.[4]

Translational mobility of ions is driven by nonpolar van der Waals (vdW) forces and electrostatic (E) interactions with the polarizable solvent.[5] The total force acting on the ion is a sum of two components,

$$\mathbf{F} = \mathbf{F}_{\rm vdW} + \mathbf{F}_E. \tag{2}$$

These two forces were viewed as statistically independent in the Born formulation[5] of dielectric friction. In this standard formulation,

$$\langle(\delta\mathbf{F})^2\rangle = \langle(\delta\mathbf{F}_{\rm vdW})^2\rangle + \langle(\delta\mathbf{F}_E)^2\rangle, \tag{3}$$

and the friction coefficient in Eq. (1) is additive, $\zeta = \zeta_{\rm vdW} + \zeta_E$. The assumption of additivity was later shared by most modern analytical theories of dielectric friction,[6–9] which followed Born's paper. More recent MD simulations have put this approximation in doubt indicating significant cross correlations between electrostatic and nonpolar (vdW) random forces.[10–15] The force variance in the Kirkwood expression should, thus, include two self-components and a cross correlation term,

$$\langle(\delta\mathbf{F})^2\rangle = \langle(\delta\mathbf{F}_E)^2\rangle + \langle(\delta\mathbf{F}_{\rm vdW})^2\rangle + 2\langle\delta\mathbf{F}_E\cdot\delta\mathbf{F}_{\rm vdW}\rangle. \tag{4}$$

A surprisingly simple relation was recently found in simulations of small dipolar solutes,[16] proteins,[17,18] and colloidal nanoparticles.[19] It allows one to relate the cross correlation between vdW and electrostatic forces to the negative of the electrostatic force variance,

$$\langle\delta\mathbf{F}_E\cdot\delta\mathbf{F}_{\rm vdW}\rangle = -\langle(\delta\mathbf{F}_E)^2\rangle. \tag{5}$$

The variance of the total force acting on a tagged particle becomes the result of subtraction of the vdW and electrostatic self-components,

$$\langle(\delta\mathbf{F})^2\rangle = \langle(\delta\mathbf{F}_{\rm vdW})^2\rangle - \langle(\delta\mathbf{F}_E)^2\rangle. \quad (6)$$

This formula replaces additivity of vdW and electrostatic force variances in the Born picture [Eq. (3)]. Equation (6) applies to solutes in water characterized by hydration shells tightly bound by the solute–solvent interactions such that random rotations of the solute drag its hydration shell with it[18] (see below for a more detailed explanation).

Here, we present MD evidence that the phenomenology of strong correlations between vdW and electrostatic forces applies to simple ions interacting with force-field (SPC/E) water by electrostatic and Lennard-Jones (LJ) forces. The generic vdW (London) interaction is, thus, replaced with the model binary LJ solute–solvent potential in our simulations. No ionic atmosphere, and friction associated with it, is included. The results presented here apply, therefore, to the limit of infinite ionic dilution. The force field of water and the solute–solvent interaction are given by binary interaction potentials. Multi-body London and induction interactions[20–22] are not a part of the model. The SPC/E force field is nonpolarizable, and electronic induced dipoles of either the solute or the solvent molecules are not included. Electronic polarizability in dense molecular liquids can often be accounted for by mean-field models operating in terms of an effective solvent dipole moment,[23,24] which becomes inhomogeneous for interfacial phenomena. Explicit simulations with polarizable force fields[20,25] are required to test this approximation in application to ionic diffusion. Diffusion coefficients of hydrated ions are typically consistent between polarizable and nonpolarizable models of water.[20,26]

The strength of the solute–solvent electrostatic interaction is altered in our simulations by varying the charge q of a spherical ion in the range $-3 \le q/e \le 3$; e is the elementary charge. The LJ radius is kept constant at $a = 2.2$ Å for all ions. The first maximum of the ion–oxygen pair distribution function is reached at $r_{\rm max} \simeq 3.6$ Å at $q/e = 1.0$. We assume that the Kirkwood equation applies to translational diffusion, which requires the solute to be much heavier than the solvent. Since the force relaxation time τ_F in Eq. (1) turns out to be little affected by the ionic charge, the dependence of D on q in Eq. (1) arises from the force variance.

The main focus of this study is on correlations between vdW and electrostatic forces. We start with the electrostatic component by considering the statistics of electrostatic potential and field at the position of the ion's charge. The electrostatic field at the center of the cavity carved by the ion defines the electrostatic force. The mean electrostatic potential specifies the interface charge, which, added to the ionic charge, yields the effective solute charge producing the screened electrostatic potential in the medium. We then turn to the statistics of vdW and electrostatic forces in terms of wavevector-dependent charge and density structure factors of the bulk liquid. The statistics of forces turn out to be asymmetric between anions and cations. Equation (6) holds well for cations, while a modification of this equation, discussed below, is required for anions.

II. POTENTIAL AND FIELD

Electrostatics of hydrated ions is characterized by the average electrostatic potential $\langle\phi_s\rangle$ produced by polarized water at the ion center and by higher moments of the electric field; the average field is zero by symmetry. The linear response approximation (LRA) anticipates[27] $\langle\phi_s\rangle \propto q$, the electrostatic interaction energy equal to $q\langle\phi_s\rangle$, and the free energy of electrostatic solvation becoming $(q/2)\langle\phi_s\rangle$. Varying the ionic charge allows us to test these predictions.

The average potential from MD simulations was corrected for finite-size effects of the Ewald sum protocol (see the supplementary material).[28,29] The resulting dependence of $\langle\phi_s\rangle$ on q is a combination of two linear branches, as anticipated from the LRA but with different slopes corresponding to different solvation susceptibilities $\chi_s = \langle\phi_s\rangle/q$ in response to anions and cations [Fig. 1(a)]. This result, documented in the past,[30–33] reflects higher solvation strength for anions compared to cations of the same absolute charge and size. The electrostatic solvation free energies are higher in magnitude for anions.

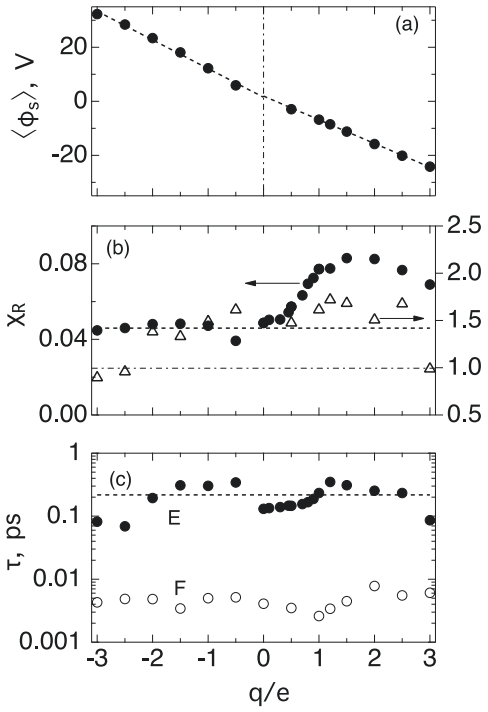

FIG. 1. (a) Average potential of water inside the spherical ion vs the ionic charge q. The linear slopes of $\langle\phi_s\rangle$ vs q for negative and positive charges are −10.62 and −8.77 V/e, respectively; the vertical dashed-dotted line is drawn to guide the eye. (b) The reaction-field susceptibility χ_R (filled circles, left axis) and the non-Gaussian parameter χ_G (open triangles, right axis) vs q. The horizontal dashed line marks the microscopic LRA calculation for χ_R from Ref. 15, the dashed-dotted line indicates the LRA result for χ_G. (c) Relaxation times of the electric field (E, filled circles) and total force (F, open circles) correlation functions. The dashed line indicates the dielectric relaxation time τ_E^c.

The physical reason for asymmetry of $\langle\phi_s\rangle$ vs q is the asymmetry of the molecular charge of water leading to a large molecular quadrupole tensor[34,35] $\mathbf{Q}$ gauged by the reduced scalar quadrupole[34] $(Q^*)^2 = 2\beta\mathbf{Q}:\mathbf{Q}/(3\sigma_s^5)$; σ_s is the water molecular diameter, and tensor contraction is used to produce the scalar. Water's reduced quadrupole Q^* is one of the largest among molecular solvents[36] and quadrupolar polarization is a significant component of water's interfacial electrostatics.[37–39] Solvation in dipolar solvents is invariant to simultaneous inversion of the ionic charge, $q \to -q$, and of the solvent dipoles, $\mathbf{m} \to -\mathbf{m}$. Molecular inversion, leading to the flipping of the dipole, leaves $\mathbf{Q}$ invariant, thus breaking the symmetry of the problem with respect to the sign of q existing in dipolar solvents. Differences in solvation of cations and anions arise from the lack of the inversion antisymmetry of the quadrupolar tensor. Solvation in purely quadrupolar solvents scales as[40] $\propto y_Q q^2$, where $y_Q = (2\pi/5)(Q^*)^2\rho^*$, $\rho^* = \rho\sigma_s^3$, and ρ is the solvent number density. It does not carry the asymmetry with respect to the ionic charge. It is the interaction between dipoles and quadrupoles that breaks the symmetry and makes anions more favorably solvated.[33]

Not only the asymmetry of the average potential vs q [Fig. 1(a)] can be traced to a large molecular quadrupole of water. Another signature of water's quadrupole is the observation of a nonzero average electrostatic potential at $q = 0$. It is caused by the spontaneous polarization of the hydration shell around a spherical cavity.[38,39,41,42] For ions studied here, the average potential extrapolates to $\langle\phi_s^0\rangle \simeq 1.94$ V at $q = 0$ for the solute–solvent excluded radius $a \simeq 3.6$ Å [Fig. 1(a)]. This number significantly exceeds the cavity electrostatic potential of $\langle\phi^c\rangle \simeq 0.3$–$0.4$ V calculated from simulations of LJ solutes of comparable size[39,43] (this should be distinguished from the cavity potential measured relative to vacuum, which includes cavity-liquid and liquid–vapor interfaces[44]). Ionic charge alters the structure of interfacial water resulting in a higher extrapolated cavity potential. Assuming that the cavity potential $\langle\phi^c\rangle = q^{st}/a$ is created by the spontaneously induced static interface charge q^{st}, one gets $q^{st} \simeq 0.49e$, which is more than a factor of 5 higher than corresponding values for LJ solutes of similar size in water.[45] This observation implies that the net electrostatic potential at the center of an uncharged solute[38,39] is hardly transferrable to calculations of ion solvation thermodynamics for that the term $q\langle\phi_s^0\rangle$ provides a linear in charge shift of the solvation free energy.

An enhancement of the interface charge of a structured polarized interface carries direct relevance to the interface-screened ionic charge q' producing the electrostatic potential q'/r in the bulk. The screened charge[45] $q' = q + q_b + q^{st}$ includes the bound charge[46] $q_b \propto q$ induced in the medium by the ion. It becomes $q' = q/\epsilon$ if $q^{st} = 0$ and continuum electrostatics is applied to define $q_b = -q(1 - \epsilon^{-1})$ from the polarized dielectric interface with the dielectric constant ϵ. The existence of q^{st}, characterizing the spontaneously polarized interface, means that even a neutral solute carries a nonzero effective interface charge.[45] Simulation results shown in Fig. 1(a) indicate that this spontaneous interface charge is substantially higher for an interface restructured by an ion compared to estimates based on simulations of partially dewetted surfaces of neutral solutes.

The asymmetry of $\langle\phi_s\rangle$ vs q also implies that a colloidal particle with positive and negative surface charges that sum up to a zero total charge will end up having a nonzero interface charge. It comes as a result of an incomplete cancellation of interface charges assigned to positive and negative ionic sites at the surface. Specific interactions, such as charge-transfer bonding,[47,48] between the colloidal particle and water will further modify q^{st} contributing to q'.

The electrostatic force $\mathbf{F}_E = q\mathbf{E}_s$ acting on the ion is the product of the ionic charge and the electrostatic field $\mathbf{E}_s$ of the polarized solvent at the position of the charge. The variance of the electrostatic force is expected to scale $\propto q^2$ in the LRA assuming that the structure of the hydration shell is not affected by the solute–solvent electrostatic interaction. (The repulsive core of the solute produces a nonlinear effect on the solute–solvent density profile, which cannot be accounted for by the LRA.[49]) Adopting the LRA assumption that the solute–solvent density profile is not altered by the electrostatic interaction, the electric field variance is expected to be independent of the ionic charge.

The LRA prediction is well supported by simulations of anions, but an upward deviation from the LRA is found for cations [Fig. 1(b)]. The field variance is quantified by the unitless reaction-field susceptibility,[15]

$$\chi_R = (\beta/6)\langle(\delta\mathbf{E}_s)^2\rangle. \tag{7}$$

The dashed line in Fig. 1(b), which agrees well with the simulation results for anions, shows χ_R calculated from an analytical microscopic theory of solvation based on the LRA.[15] On the other hand, there is an increase in χ_R with the increasing cationic charge. This phenomenology must be related to a structural change in the hydration shell caused by the cation and violating the basic assumption of the LRA. Cations pull water oxygens in the first hydration layer and force the O–H bonds to reorient into the bulk. This structural reorganization of the hydration shell is reflected in a nonlinear dependence of χ_R on q. Note that the density profile around ions, both cations and anions, for SPC/E water used here is consistent with quantum density functional theory (DFT) calculations.[50] Given that the interaction energy of the ion with the water dipoles scales as qm/r, one can anticipate the appearance of similar maxima at comparable q/a values for cations with different radii a.

An asymmetry between anions and cations is also seen in the density profile of water around the ion. Figure 2 shows the dependence of the height of the first maximum $G_{0s} = g_{0s}(r_{max})$ of the solute–oxygen pair distribution function $g_{0s}(r)$ on the ionic charge. Anions are overall more efficient in compressing water since more

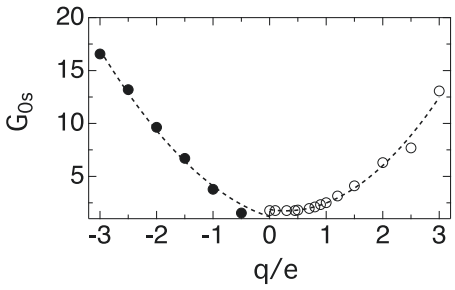

FIG. 2. Magnitude of the first peak $G_{0s} = g_{0s}(r_{max})$ of the ion–oxygen pair distribution function $g_{0s}(r)$ vs the ionic charge q; SPC/E water at $T = 300$ K. Dashed lines are fit through the points calculated from MD drawn to guide the eye.

efficient packing and higher density is achieved in this case by releasing dangling O–H bonds[51] pointing toward the negative charge of the ion.

The LRA also stipulates the fluctuation-dissipation[52] relation between the first and second moments of the electrostatic ion–solvent interaction energy,[27,53] $\chi_G = -\beta q\langle(\delta\phi_s)^2\rangle/\langle\phi_s\rangle = 1$. Deviations from $\chi_G = 1$ quantify the extent of the non-Gaussian character of electrostatic fluctuations. The parameter χ_G [Fig. 1(b)] roughly follows the reaction-field susceptibility χ_R, indicating that the same physical reasons, rooted in the hydration shell restructuring, are responsible for deviations from both LRA relations, $\chi_R = Const$ and $\chi_G = 1$. None of these microscopic details are reflected in the average electrostatic potential $\langle\phi_s\rangle$, which shows a perfectly linear scaling with q consistent with the LRA.

III. FORCE

Figure 1(c) shows the integral relaxation times calculated from the time autocorrelation functions for the electrostatic (E) force (τ_E) and the total (F) force (τ_F),

$$C_a(t) = \langle\delta\mathbf{F}_a(t)\cdot\delta\mathbf{F}_a(0)\rangle, \quad \text{a} = \text{E, F}. \tag{8}$$

The horizontal line in Fig. 1(c) marks the prediction of dielectric theories,[54] $\tau_E^c = 3\tau_D/(2\epsilon+1)$, where τ_D is the Debye relaxation time of the polar solvent[55] (10.4 ps for SPC/E water at 300 K[15]). Tightening of the hydration shell caused by increasing the magnitude of the ionic charge does not strongly affect relaxation times. One, thus, anticipates that the dependence of the diffusion constant on the ionic charge [Eq. (1)] comes from the force variance. Both the total force variance and its electrostatic and vdW components scale approximately linearly with q^2 (Fig. 3).

The variance of the electrostatic force is conveniently represented in terms of the charge–charge structure factor[2,56] $S_{qq}(k)$ by converting calculations from direct to reciprocal space. One obtains the following expression (see the supplementary material):

$$\langle(\delta\mathbf{F}_E)^2\rangle = 3\rho q^2\int\frac{d\mathbf{k}}{(2\pi)^3}\left|\tilde{\boldsymbol{E}}_0(\mathbf{k})\right|^2 S_{qq}(k), \tag{9}$$

where $\rho = N/V$ is the number density of N water molecules occupying the volume V and $\tilde{\mathbf{E}}_0$ is the Fourier transform of the electric field of the ion carrying the unit charge weighted with the solute–solvent density profile represented by the solute–solvent (ion–oxygen here) pair correlation function $g_{0s}(r)$,

$$\tilde{\mathbf{E}}_0(\mathbf{k}) = e\int\mathbf{r}g_{0s}^{1/2}(r)e^{i\mathbf{k}\cdot\mathbf{r}}(d\mathbf{r}/r^3). \tag{10}$$

The charge–charge structure factor[2] represents correlated fluctuations of the water charge density probed at the length scale specified by the wavevector k,

$$S_{qq}(k) = \frac{1}{3N}\sum_{i,j,\alpha,\beta}\left\langle z_\alpha z_\beta e^{i\mathbf{k}\cdot(\mathbf{r}_{i\alpha}-\mathbf{r}_{j\beta})}\right\rangle, \tag{11}$$

where the sum runs over $i,j = 1,\ldots,N$ water molecules and α, $\beta = 1,2,3$ atoms of each water molecule carrying the partial charges $z_{\alpha,\beta}$. The structure factor shows no compressibility of the charge density[2] at $k\to 0$ yielding $S_{qq}(k\to 0)\to 0$. The leading expansion term $S_{qq}(k)\simeq(\Lambda k)^2$ is linear in k^2. The length parameter Λ follows from the Lemberg–Stillinger equation[57] $\Lambda^2 = \chi^L/(3\beta\rho e^2)$ with $\chi^L = (\epsilon-1)/(4\pi\epsilon)$ representing the longitudinal susceptibility of the polar liquid. The opposite asymptote, at $k\to\infty$, is nonzero,

$$S_{qq}(k\to\infty)\to\frac{1}{3}\left[z_O^2+2z_H^2\right], \tag{12}$$

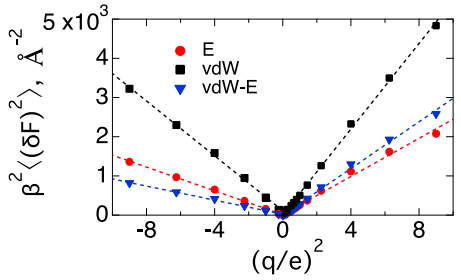

FIG. 3. Force variance components vs q^2: vdW (black), electrostatic (red), and the negative of cross-vdW-electrostatic (blue). The results for anions are plotted vs $-q^2$. The dashed lines are linear fits through the points.

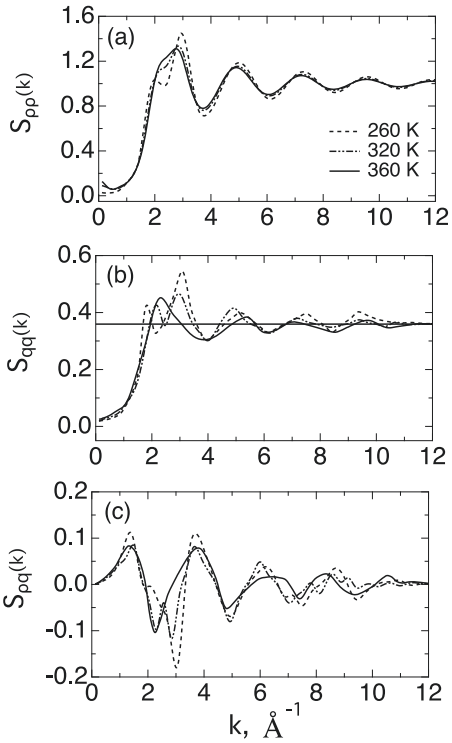

FIG. 4. (a) $S_{\rho\rho}(k)$ [Eq. (16)], (b) $S_{qq}(k)$ [Eq. (11)], and (c) $S_{\rho q}(k)$ [Eq. (18)] for SPC/E water at the temperatures listed in the plot. The horizontal line in (b) refers to the $k\to\infty$ asymptote specified by Eq. (12).

where $z_O = z_1$ and $z_H = z_2 = z_3$ are the atomic partial charges of the water molecule. This limit is shown by the straight horizontal line in Fig. 4(b), where the structure factors $S_{qq}(k)$ from MD simulations of SPC/E water are shown at three temperatures (see the supplementary material for the simulation protocol and additional temperatures).

Reciprocal-space integration in Eq. (9) accounting for $k \to 0$ and $k \to \infty$ limits (see the supplementary material) suggests that electrostatic friction ζ_E, which can be associated with the electrostatic force component in Eqs. (1) and (3), is roughly proportional to the product of ion's solvation free energy F_q and the field relaxation time τ_E and carries an addition inverse proportionality to the ionic radius a,

$$\zeta_E \propto \tau_E F_q a^{-1}. \tag{13}$$

Given that $F_q \propto a^{-1}$ in the Born solvation model, the electrostatic friction applied to a center charge decays as a^{-2} and becomes less significant for large ions. This conclusion does not apply to colloidal particles stabilized in solution by surface solvation.

The solute–solvent vdW force is given by a sum of binary forces $\mathbf{f}_{\rm vdW}(i)$ with each molecule of the solvent (no multi-body effects[20–22] are included). The vdW interactions are modeled by the LJ solute–solvent potential in simulations, and we write

$$\mathbf{F}_{\rm vdW} = \sum_i \mathbf{f}_{\rm LJ}(i). \tag{14}$$

The variance of the force can be expressed in terms of the density–density structure factor $S_{\rho\rho}(k)$ upon transforming to reciprocal space (see the supplementary material),

$$\langle (\delta \mathbf{F}_{\rm vdW})^2 \rangle = 3\rho \int \frac{d\mathbf{k}}{(2\pi)^3} \left| \tilde{\mathbf{f}}_{\rm LJ}(\mathbf{k}) \right|^2 S_{\rho\rho}(k). \tag{15}$$

The density–density structure factor[2] represents correlated fluctuations of density in the bulk and is given by the following relation, which does not involve atomic charges z_α appearing in $S_{qq}(k)$ in Eq. (11),

$$S_{\rho\rho}(k) = \frac{1}{3N} \sum_{i,j,\alpha,\beta} \left\langle e^{i\mathbf{k}\cdot(\mathbf{r}_{i\alpha} - \mathbf{r}_{j\beta})} \right\rangle. \tag{16}$$

In addition, the spatial Fourier transform of the solute–solvent LJ force in Eq. (15) becomes

$$\tilde{\mathbf{f}}_{\rm LJ}(\mathbf{k}) = \int d\mathbf{r}\, g_{0s}^{1/2}(r) \mathbf{f}_{\rm LJ}(r) e^{i\mathbf{k}\cdot\mathbf{r}}. \tag{17}$$

The vdW force varies steeply with the solute–solvent distance in direct space, which implies that its Fourier transform is a slowly changing function of the wavevector. The reciprocal-space integral in Eq. (15) can be evaluated in the continuum limit $S_{\rho\rho}(k) \simeq S_{\rho\rho}(0)$ for the density structure factor,

$$\langle (\delta \mathbf{F}_{\rm vdW})^2 \rangle = 12\pi\rho S_{\rho\rho}(0) \int_0^\infty dr r^2 g_{0s}(r) f_{\rm LJ}^2(r). \tag{18}$$

The function $r^2 g_{0s}(r) f_{\rm LJ}^2(r)$ peaks sharply near the maximum of the solute–solvent pair distribution function $g_{0s}(r)$ (Fig. S4), and the integral in Eq. (18) scales linearly with the height of the first peak $G_{0s} = g_{0s}(r_{\rm max})$ of the solute–solvent pair distribution function (Fig. 5),

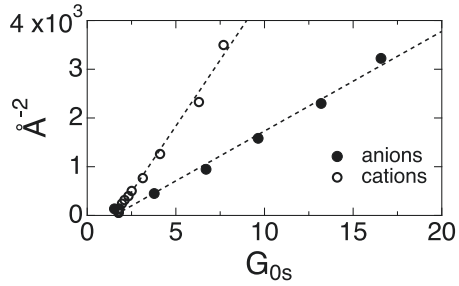

FIG. 5. Variance of the vdW force $\beta^2 \langle (\delta \mathbf{F}_{\rm vdW})^2 \rangle$ (Å^{-2}) vs $G_{0s} = g_{0s}(r_{\rm max})$ (see Fig. 2).

$$\langle (\delta \mathbf{F}_{\rm vdW})^2 \rangle \propto G_{0s}. \tag{19}$$

This scaling suggests that a linear dependence of $\langle (\delta \mathbf{F}_{\rm vdW})^2 \rangle$ on q^2 (Fig. 3) is caused by tightening of the hydration shell induced by the electrostatic pull from the ion.

The cross correlation between electrostatic and vdW forces can be related to the mixed, charge-density structure factor[58] [Fig. 4(c)],

$$S_{\rho q}(k) = \frac{1}{3N} \sum_{i,j,\alpha,\beta} \left\langle z_\alpha e^{i\mathbf{k}\cdot(\mathbf{r}_{i\alpha} - \mathbf{r}_{j\beta})} \right\rangle. \tag{20}$$

This structure factor tends to zero at both $k \to 0$ and $k \to \infty$ because of electroneutrality of the polar liquid.

Common to all structure factors of water is the disappearance of the double-maximum structure of the first peak at higher temperatures and the merger of these two maxima into a single peak (We also find the previously reported minimum of the density structure factor at small k at lower temperatures.[59,60]). The single-peak structure factor is typical for simple liquids. Water thus structurally converges to the behavior of a simple polar liquid, both in terms of density and charge fluctuations, at $T > 320$ K. This structural crossover is potentially reflected by solvation and other observable properties. The distribution of tetrahedral order parameter[61] of water in hydration shells of ions[62] and Raman O–H stretch in hydration shells of sufficiently long linear alcohols[51,63] all show distinct crossovers in this temperature range.

The theoretical arguments expressing the force variance and cross correlations in terms of k-dependent structure factors of the bulk liquid are not intended to provide a quantitative solution to the problem of dielectric friction. Rather, they are presented to arrive at general scaling relations for self-variances with the parameters of the problem [Eqs. (13) and (19)]. The advantage of the reciprocal-space representation is that the $k \to 0$ limit produces results in terms of collective properties of the medium, involving multi-body correlations, which are not reducible to single–molecule parameters. Nevertheless, there are quantitative difficulties with the present formalism. For instance, Eq. (18) does not explain different slopes of the vdW variance vs G_{0s} in Fig. 5. Quantitative theories are still required for a complete grasp of the complex problem of dielectric friction.

IV. DISCUSSION

The Born picture[5] of dielectric friction adopted in many modern formulations is based on two assumptions: (i) friction due to vdW forces is described by hydrodynamic drag and is independent of the ionic charge and (ii) vdW and electrostatic forces are statistically independent. Both assumptions turn out to be incorrect for LJ ions studied here: the variances of both vdW and electrostatic forces scale linearly with q^2, and there is a strong anticorrelation (negative cross correlation) between them.

The present set of simulations provides us with a broad view of correlations between vdW and electrostatic forces kicking, by thermal agitation, cations and anions into random translational diffusion. The results for the self-components of the force variance and the cross correlations are shown in Fig. 3 (the numerical results are listed in the supplementary material). The component forces are compared on the logarithmic scale with the total force variance in Fig. 6. The equality between the cross correlation term and the negative of the self-electric component, given by Eq. (5), holds more accurately for cations than for anions. For cations, the cross correlation falls slightly above the electrostatic component, while just the opposite happens for anions. As a result, Eq. (6) for the total variance holds reasonably well for cations, but an even simpler result applies to anions (Fig. 6, compare orange diamonds with black squares for anions),

$$\langle(\delta\mathbf{F})^2\rangle \simeq \langle(\delta\mathbf{F}_{\rm vdW})^2\rangle. \tag{21}$$

The physical reason for the equality between the electrostatic self-variance and the negative of the cross correlation [Eq. (5)] is the formation of a tightly bound hydration layer. When the solute is either nonspherical or carries an asymmetric charge distribution, the tightly bound hydration shell rotates with the solute.[16] For a water molecule in such a structured hydration layer, mechanical equilibrium between vdW and electrostatic solute–solvent forces holds in the body frame of the solute, $\tilde{f}_{\rm vdW} = -\tilde{f}_E$, where tildes denote the solute body frame and projection on the radial direction is taken to produce the scalar solute–solvent forces acting on a single water molecule. If the molecule in the shell is structurally arrested and rotates with the solute,[24] the fluctuation of the force in the laboratory frame (without tildes) is produced by the orientation of the radial unit vector changing with solute's rotation: $\delta\mathbf{f}_{\rm vdW} = -\hat{\mathbf{r}}\tilde{f}_E$ and $\delta\mathbf{f}_E = \hat{\mathbf{r}}\tilde{f}_E$. This condition immediately leads to the compensation relation in Eq. (5).

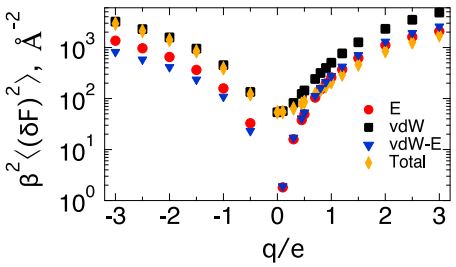

FIG. 6. Variances of vdW (black squares) and electrostatic (red circles) interactions and the cross correlation $-\langle\delta\mathbf{F}_E \cdot \delta\mathbf{F}_{\rm vdW}\rangle$ (vdW-E, blue triangles). Orange points, nearly coinciding with the vdW component for anions, refer to the total force variance.

Similar qualitative arguments apply to spherical ions studied here. Mechanical equilibrium for a water molecule in the hydration layer implies that fluctuations of vdW and electrostatic forces roughly compensate each other, $\delta f_E = -\delta f_{\rm vdW}$, which leads to Eq. (6). One also has to stress that the solvent molecule does not have to continuously reside within the shell and can exchange with another solvent molecule in the bulk. It is the structure of the shell, induced by the ion, which has to be maintained.

We find that all three components of the force variance in Eq. (4) approximately follow linear scalings with q^2 (Fig. 3), despite some deviations from the LRA seen for cations [Fig. 1(b)]. Given that τ_F in Eq. (1) is nearly independent of the ionic charge [Fig. 1(c)], the inverse diffusion constant is predicted to follow a linear scaling with the squared ionic charge,

$$D^{-1} = a + bq^2, \tag{22}$$

for simple ions in water. The linear slope b is higher for anions than that for cations because of the distinction between Eqs. (6) and (21). The solvation asymmetry [Fig. 1(a)], thus, extends to the asymmetry of linear transport coefficients: according to the Kirkwood equation [Eq. (1)] and the values of force variances (Fig. 6), cations should diffuse faster than anions of the same size and charge magnitude.

In contrast to the present findings for simple LJ ions, diffusion constants of proteins turn out to be little affected by charge mutations.[17] Stabilization of proteins and other colloidal particles in solution is achieved by surface solvation of many surface ionic sites (ionized residues for proteins) making up the overall solute charge. Small alterations of the charge state of a few such surface sites do not strongly affect diffusivity. The transition from high sensitivity of translational diffusion to the ionic charge demonstrated here for small spherical ions to the lack of such sensitivity for colloidal particles, and the study of intermediate length scales, will remain the subject for future studies.

SUPPLEMENTARY MATERIAL

See the supplementary material for the simulation protocol, structure factors of SPC/E water, and derivations of equations presented in the text.

ACKNOWLEDGMENTS

This research was supported by the National Science Foundation (Grant No. CHE-2154465), XSEDE resources (Grant No. TG-MCB080071) and ASU's Research Computing.

AUTHOR DECLARATIONS

Conflict of Interest

The authors have no conflicts to disclose.

DATA AVAILABILITY

The data that support the findings of this study are available within the article and its supplementary material.

REFERENCES

[1] R. Zwanzig, Annu. Rev. Phys. Chem. **16**, 67 (1965).
[2] J.-P. Hansen and I. R. McDonald, *Theory of Simple Liquids*, 4th ed. (Academic Press, Amsterdam, 2013).
[3] U. Balucani and M. Zoppi, *Dynamics of the Liquid Phase* (Clarendon Press, Oxford, 1994).
[4] H. K. Shin, C. Kim, P. Talkner, and E. K. Lee, Chem. Phys. **375**, 316 (2010).
[5] M. Born, Z. Phys. **1**, 221 (1920).
[6] T. W. Nee and R. Zwanzig, J. Chem. Phys. **52**, 6353 (1970).
[7] R. Zwanzig, J. Chem. Phys. **52**, 3625 (1970).
[8] J. Hubbard and L. Onsager, J. Chem. Phys. **67**, 4850 (1977).
[9] P. G. Wolynes, Annu. Rev. Phys. Chem. **31**, 345 (1980).
[10] M. Berkowitz and W. Wan, J. Chem. Phys. **86**, 376 (1987).
[11] S. Koneshan, J. C. Rasaiah, R. M. Lynden-Bell, and S. H. Lee, J. Phys. Chem. B **102**, 4193 (1998).
[12] S.-H. Chong and F. Hirata, J. Chem. Phys. **108**, 7339 (1998).
[13] P. V. Kumar and M. Maroncelli, J. Chem. Phys. **112**, 5370 (2000).
[14] J. C. Rasaiah and R. M. Lynden-Bell, Philos. Trans. R. Soc., A **359**, 1545 (2001).
[15] T. Samanta and D. V. Matyushov, J. Chem. Phys. **153**, 044503 (2020).
[16] T. Samanta and D. V. Matyushov, Phys. Rev. Res. **3**, 023025 (2021).
[17] S. M. Sarhangi and D. V. Matyushov, J. Phys. Chem. Lett. **11**, 10137 (2020).
[18] T. Samanta, S. M. Sarhangi, and D. V. Matyushov, J. Phys. Chem. Lett. **12**, 6648 (2021).
[19] A. Y. Cui and Q. Cui, J. Phys. Chem. B **125**, 4555 (2021).
[20] D. Spångberg and K. Hermansson, J. Chem. Phys. **120**, 4829 (2004).
[21] A. Ambrosetti, N. Ferri, R. A. DiStasio, Jr., and A. Tkatchenko, Science **351**, 1171 (2016).
[22] F. Réal, V. Vallet, and M. Masella, J. Comput. Chem. **40**, 1209 (2019).
[23] G. Stell, G. N. Patey, and J. S. Høye, Adv. Chem. Phys. **48**, 183 (1981).
[24] D. Jiao, C. King, A. Grossfield, T. A. Darden, and P. Ren, J. Phys. Chem. B **110**, 18553 (2006).
[25] A. Grossfield, P. Ren, and J. W. Ponder, J. Am. Chem. Soc. **125**, 15671 (2003).
[26] H. Yu, T. W. Whitfield, E. Harder, G. Lamoureux, I. Vorobyov, V. M. Anisimov, A. D. MacKerell, and B. Roux, J. Chem. Theory Comput. **6**, 774 (2010).
[27] G. Hummer, L. R. Pratt, A. E. García, B. J. Berne, and S. W. Rick, J. Phys. Chem. B **101**, 3017 (1997).
[28] G. Hummer, L. R. Pratt, and A. E. García, J. Chem. Phys. **107**, 9275 (1997).
[29] P. H. Hünenberger and J. A. McCammon, J. Chem. Phys. **110**, 1856 (1999).
[30] R. M. Lynden-Bell and J. C. Rasaiah, J. Chem. Phys. **107**, 1981 (1997).
[31] G. Hummer, L. R. Pratt, and A. E. García, J. Phys. Chem. A **102**, 7885 (1998).
[32] D. L. Mobley, A. E. Barber, C. J. Fennell, and K. A. Dill, J. Phys. Chem. B **112**, 2405 (2008).
[33] S. J. Cox, K. K. Mandadapu, and P. L. Geissler, J. Chem. Phys. **154**, 244502 (2021).
[34] C. G. Gray and K. E. Gubbins, *Theory of Molecular Liquids*, Fundamentals Vol. 1 (Clarendon Press, Oxford, 1984).
[35] S. Niu, M.-L. Tan, and T. Ichiye, J. Chem. Phys. **134**, 134501 (2011).
[36] D. V. Matyushov, *Manual for Theoretical Chemistry* (World Scientific Publishing Co. Pte. Ltd., NJ, 2021).
[37] M. A. Wilson, A. Pohorille, and L. R. Pratt, J. Chem. Phys. **88**, 3281 (1988).
[38] T. L. Beck, Chem. Phys. Lett. **561-562**, 1 (2013).
[39] L. Horváth, T. Beu, M. Manghi, and J. Palmeri, J. Chem. Phys. **138**, 154702 (2013).
[40] A. A. Milischuk and D. V. Matyushov, J. Chem. Phys. **123**, 044501 (2005).
[41] H. S. Ashbaugh, J. Phys. Chem. B **104**, 7235 (2000).
[42] R. C. Remsing, M. D. Baer, G. K. Schenter, C. J. Mundy, and J. D. Weeks, J. Phys. Chem. Lett. **5**, 2767 (2014).
[43] S. Rajamani, T. Ghosh, and S. Garde, J. Chem. Phys. **120**, 4457 (2004).
[44] C. C. Doyle, Y. Shi, and T. L. Beck, J. Phys. Chem. B **123**, 3348 (2019).
[45] D. V. Matyushov, Biomicrofluidics **13**, 064106 (2019).
[46] J. D. Jackson, *Classical Electrodynamics* (Wiley, New York, 1999).
[47] S. Pullanchery, S. Kulik, B. Rehl, A. Hassanali, and S. Roke, Science **374**, 1366 (2021).
[48] J. M. Herbert and K. Carter-Fenk, J. Phys. Chem. A **125**, 1243 (2021).
[49] D. Chandler, Phys. Rev. E **48**, 2898 (1993).
[50] R. C. Remsing, T. T. Duignan, M. D. Baer, G. K. Schenter, C. J. Mundy, and J. D. Weeks, J. Phys. Chem. B **122**, 3519 (2018).
[51] J. G. Davis, K. P. Gierszal, P. Wang, and D. Ben-Amotz, Nature **491**, 582 (2012).
[52] R. Kubo, Rep. Prog. Phys. **29**, 255 (1966).
[53] D. R. Martin and D. V. Matyushov, Phys. Rev. E **78**, 041206 (2008).
[54] B. Bagchi, *Molecular Relaxation in Liquids* (Oxford University Press, Oxford, 2012).
[55] B. K. P. Scaife, *Principles of Dielectrics* (Clarendon Press, Oxford, 1998).
[56] N. H. March and M. P. Tosi, *Coulomb Liquids* (Academic Press, London, 1984).
[57] H. L. Lemberg and F. H. Stillinger, J. Chem. Phys. **62**, 1677 (1975).
[58] F. Sedlmeier, S. Shadkhoo, R. Bruinsma, and R. R. Netz, J. Chem. Phys. **140**, 054512 (2014).
[59] G. N. I. Clark, G. L. Hura, J. Teixeira, A. K. Soper, and T. Head-Gordon, Proc. Natl. Acad. Sci. U. S. A. **107**, 14003 (2010).
[60] F. Sedlmeier, D. Horinek, and R. R. Netz, J. Am. Chem. Soc. **133**, 1391 (2011).
[61] J. R. Errington and P. G. Debenedetti, Nature **409**, 318 (2001).
[62] S. M. Sarhangi, M. M. Waskasi, S. M. Hashemianzadeh, and D. V. Matyushov, Phys. Chem. Chem. Phys. **20**, 27069 (2018).
[63] X. Wu, W. Lu, L. M. Streacker, H. S. Ashbaugh, and D. Ben-Amotz, J. Phys. Chem. Lett. **9**, 1012 (2018).